Molecular layer detection on a diffractive optical balance

Xuefeng Wang, Ming Zhao, and David D. Nolte*

Department of Physics, Purdue University, West Lafayette, Indiana 47907, USA
**Corresponding author: nolte@physics.purdue.edu*

Received July 13, 2012; revised August 29, 2012; accepted August 29, 2012;
posted August 31, 2012 (Doc. ID 168341); published September 26, 2012

Diffraction-based molecular detection is achieved by etching optical gratings into thermal oxide on silicon. The gratings perform as a stable common-path diffractive optical balance (DOB) designed to operate near a missing diffraction order. The biosensor is operated in an off-null condition with a phase bias to produce a high-contrast responsivity that is linear in accumulated molecules but with a low background. The DOB linear responsivity is a factor of 20 larger than the reflectometric responsivity of planar thermal oxide.

OCIS codes: 280.1415, 240.0310, 240.3990.

Label-free interferometric biosensors have the potential for highly multiplexed assay applications because of the absence of secondary labels [1,2]. To achieve high signal-to-noise performance, interferometric optical biosensors should exhibit large linear responsivity to accumulating molecules with low background and high stability [3]. Diffraction-based biosensors have intrinsically low backgrounds because off-angle detection of diffraction orders performs as a spatial filter that eliminates the zero-order reflectance. One example of a diffraction-based biosensor used UV photoinactivation to produce periodic stripes of antigen or antibody to detect choriogonadotropin in serum [4]. Such sensors, however, with quadratic responsivity (i.e., null condition) have very low sensitivity to a thickness d of small molecules or to thin layers of even large molecules [3] because of the small value of $(d/\lambda)^2$. The diffraction signal can be increased by labeling the target molecules with gold particles [5] or by using horseradish peroxidase [6], but these enhanced sensitivity approaches are not label free.

This Letter describes a diffraction-based biosensor that has high stability, near-null background, and hence high contrast, linear sensitivity, and high signal-to-noise ratio (SNR). It is based on the principle of a missing diffraction order commonly encountered in diffraction physics that occurs when there is a balanced destructive interference of partial diffracted waves. The resulting performance is similar to near antireflection reflectometric biosensors [7–10], such as the inline BioCD [11], but with the added advantage of the off-angle spatial filtering that eliminates spurious reflectances from the optical system. Linear responsivity is achieved while retaining low background by operating in a near-null condition, which is slightly shifted from complete destructive interference conditions. The performance of the diffraction optical balance is compared with an inline BioCD.

For label-free biosensors in the case of printed gratings of biolayers on planar surfaces, there is no direct way to increase this sensitivity other than by adding large light-scattering labels, such as beads or nanoparticles [5]. In the case of the diffractive optical balance (DOB), on the other hand, it is straightforward to design the device parameters to provide a bias for the first diffraction order. The bias is introduced by slightly misbalancing the grating so that there is a nonzero initial first-order diffraction field. This locally generated bias acts as a local oscillator that establishes an interference condition with linear dependence on d/λ. Because the bias is generated locally, it is also a common-path configuration [11] and hence is stable against mechanical vibrations. This bias gives rise to the linear response to the biolayer thickness and still retains large signal-to-background ratios for DOB sensors.

The DOB is fabricated by etching parallel periodic grooves on a surface (125 grooves/mm on a thermal-oxide silicon chip with 65 nm depth). Two features are essential to realize the near-null optical balance. First, the reflection coefficients r_1 and r_2 must be nearly equal on the grating ridges and grooves to produce the initial pseudozero first-order diffraction that depends on the relation $I = \eta|r_1 - r_2|^2$, where η is the diffraction coefficient. Second, the ridges and grooves must have a proper height difference h that optimizes the diffraction change after applying the biolayer.

For a DOB grating, as shown in Fig. 1(a), the initial reflection coefficients on the ridges and the grooves of the grating are r_1 and r_2, respectively. Both are referenced to the top surface of the ridge. The reflection coefficient from the grooves (referenced to the groove floor) is r_3. The relationship between r_3 and r_2 is $r_3 = r_2 e^{i\alpha}$, where $\alpha = 4\pi n_0 h \cos\theta_0/\lambda$ is the phase delay contributed by the height difference h between the ridge and groove surfaces. After adding a molecular layer, the

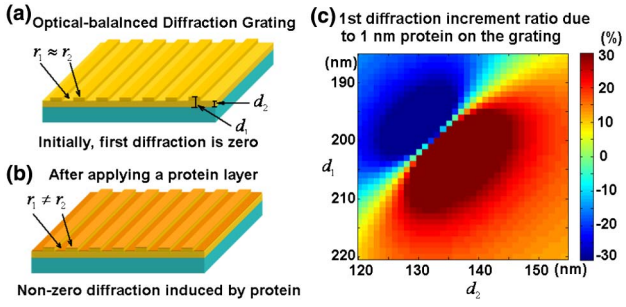

Fig. 1. (Color online) DOB grating fabricated on thermal oxide on silicon. (a) SiO_2 thicknesses on the ridges and the grooves are 205 and 140 nm, respectively; a pseudozero first-order diffraction is achieved when the grating is illuminated by normal-incidence 488 nm wavelength light. (b) A protein layer immobilized on both the ridges and the grooves increases the diffraction; the depth of the grooves is an essential parameter for a strong induced diffraction. (c) Map of linear responsivity per 1 nm protein as a function of ridge and groove thermal oxide thicknesses.

coefficients r_1 and r_2 change to r_1' and r_2', where the reference surface remains the initial ridge surface. Because the molecular layer thickness satisfies $d \ll \lambda$, the modified reflection coefficients are as follows [12]:

$$r_1' = r_1 + (1 + r_1)^2 i\delta$$
$$r_2' = r_2 + e^{-i\alpha}(1 + r_2 e^{i\alpha})^2 i\delta, \quad (1)$$

where $\delta = (n_0^2 - n_p^2)\pi d/(\lambda n_0 \cos\theta_0)$, d is the molecular thin film thickness, n_p is its refractive index, n_0 is the refractive index of the ambient medium, λ is the probe light wavelength, and θ_0 is the incidence angle. All reference surfaces remain at the initial ridge surface. For $\varepsilon = r_1 - r_2$, the initial first-order diffraction intensity is $I = \eta|\varepsilon|^2$. After the molecular layer deposition, the diffraction intensity becomes

$$I' = |r_1' - r_2'|^2 = I + \eta|B(r_1, h)|^2\delta^2 + 2\eta\,\mathrm{Im}[B(r_1, h)^*\varepsilon]\delta, \quad (2)$$

where $B(r_1, h) = 1 - e^{-i\alpha} + r_1^2(1 - e^{i\alpha})$.

At perfect balance, $\varepsilon = r_1 - r_2 = 0$, and Eq. (2) is reduced to $I' = \eta|B(r_1, h)|^2\delta^2$, which has the conventional quadratic dependence of the diffracted intensity on the thickness of the molecular layer that is characteristic of a missing diffraction order. Linear responsivity is achieved by introducing a phase bias on the grating. The bias is caused by the imbalance of Eq. (2) when ε is nonzero. For $|\delta| \ll |\varepsilon| \ll 1$ the diffracted intensity is dominated by the linear dependence on the biolayer thickness through the third term in Eq. (2), which is the heterodyne term. As ε goes to zero, this linear term vanishes and the quadratic response is recovered. The design challenge for a DOB biosensor is to set a finite ε that produces sufficiently low background but with high sensitivity to biolayer coverage.

A DOB surface based on thermal oxide on silicon requires only a single step of SiO_2 etching. Grooves with 8 μm periodicity and 65 nm height were etched on a SiO_2/Si chip with 20 mm × 20 mm area on a 200 nm SiO_2 thermal oxide on silicon [shown in Fig. 1(a)] using photolithography. The first-order diffraction angle is 3.5 deg at normal incidence for a 488 nm probe laser. The theoretical biosensor linear responsivity is plotted in Fig. 1(c) as a function of the ridge and groove thermal oxide thicknesses d_1 and d_2. The linear sensitivity vanishes for the perfect balance condition but near the fabricated SiO_2 thicknesses of 205/140 nm for the ridges and grooves, respectively, demonstrated in this paper, the theoretical protein response is 40% for 1 nm protein.

A laser scanning BioCD system [2] was designed and constructed to perform protein array imaging of the DOB surface, shown in Fig. 2. The incident angle is tilted from the surface-normal direction so that the first-order diffraction beam from the DOB chip is diffracted, counterpropagating to the path of the incidence beam. The tilted angle is 1.75 deg, which is half of the first-order diffraction angle, and the laser divergence angle was small (1.26 deg), allowing the diffraction to be separated from the reflected beam. In this configuration, the interferometry is common path and stable, and specular reflections

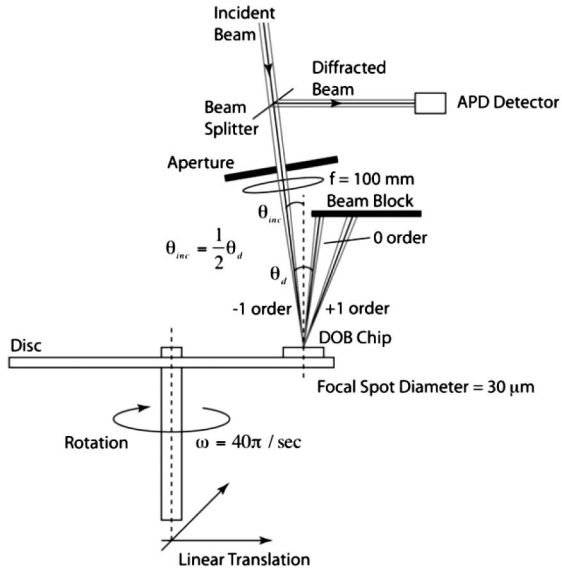

Fig. 2. Common-path laser scanning BioCD system based on first-order diffraction from the DOB chip. The laser is not incident perpendicular to the disc, but it is tilted by half the diffraction angle. This permits the −1st-order diffraction to counterpropagate through the pinhole, which serves as a spatial filter that automatically demodulates the spatial carrier wave of the grating.

are eliminated. A pinhole is placed after the objective lens ($f = 100$ mm) to block the other diffraction orders. The DOB chip was attached to a supporting disk placed on a motor spinning at 20 Hz on a linear translation stage. The motor and the linear stage form a polar coordinate system to perform two-dimensional mapping. A detector with sensitivity 1.5×10^6 V/W was used for light detection for a typical power of the first-order diffraction in our experiments in the range of 0.1–1 μW for a 488 nm probe laser power around 10 mW.

We first tested protein immobilization and imaging on the DOB surface. By physical adsorption, rabbit IgG (I5006, Sigma Inc.) was spotted on the chip surface forming a protein monolayer. By detecting the diffraction from the DOB surface and rejecting the specular reflection, the data are automatically demodulated from the carrier frequency (the grating) through spatial filtering. This detection of the diffracted signal is the demodulation process, and no other analysis or algorithm is required. The results are shown in Fig. 3(b), showing that the protein was successfully immobilized, and the image has been demodulated with no residual spatial carrier frequency caused by the 8 μm periodicity of the grating when probed by a focal spot with a 15 μm radius. Because a SiO_2 surface is a general surface for gene and protein arrays, the DOB grating based on a silicon wafer is compatible with many surface chemistries for biomaterial immobilization.

To calibrate the DOB surface response, we fabricated 1 nm high SiO_2 spots (which have a refractive index similar to protein) on a DOB surface and on a conventional inline BioCD surface, which is a 120 nm SiO_2/Si wafer. The process etched the background SiO_2 by 1 nm except in the spot regions. The spots on the DOB surface and on the inline BioCD were processed under the same

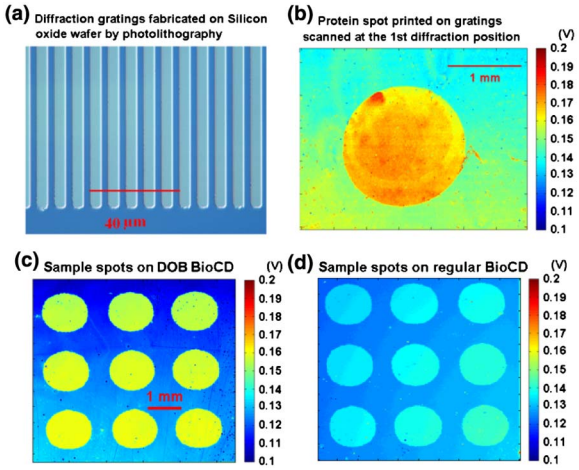

Fig. 3. (Color online) (a) Optical micrograph of the gratings produced by photolithography. (b) IgG antibody spot immobilized on the grating scanned and automatically demodulated from the carrier frequency in the image. (c) and (d) Spot arrays created on the DOB grating and on a BioCD by a second round of photolithography with precise 1 nm SiO_2 thickness to simulate protein spots and calibrate the DOB sensitivity. The linear responsivity is 50% per nm on the DOB and is 2.5% per nm on a reflectometric BioCD.

conditions, and the spot thicknesses were identical. The imaging results are shown in Figs. 3(c) and 3(d). The intensity increment due to 1 nm SiO_2 is 50% on the DOB and is only 2.5% on a reflectometric BioCD [11], which is an improvement in linear responsivity of a factor of 20. The SNR is the signal increment on the spots divided by the standard deviation of the background. The SNR is equal to 26 for the DOB and is equal to 6 for the reflectometric BioCD. Therefore, the SNR is improved by a factor of 4, with further improvements possible through appropriate design and fabrication. Using the silica spot as a calibration, the protein thickness in Fig. 3(b) is inferred to be around 0.6 nm assuming protein and silica having similar refractive indexes.

In conclusion we have presented the concept of a DOB surface, fabricated a prototype of the DOB based on a SiO_2 /Si wafer, and constructed a common-path laser scanning system to image immobilized protein using the diffraction signal. We calibrated the responsivity with SiO_2 spots for precise thickness control. A 1 nm SiO_2 layer induces a 50% signal increment, which is 20 times larger than a reflectometric inline BioCD. The combined off-null and off-angle operation of the DOB give it low background and high contrast while simultaneously eliminating specular reflections. It is compatible with high-speed laser scanning and imaging in which the DOB chips are attached to a spinning BioCD, with the potential for high multiplexing bioassay applications in the future.

This work was sponsored under grants from Quadraspec, Inc., from the Indiana Economic Development Corporation through the Purdue Research Foundation, and National Institutes of Health awards 5R21CA125336-02 and 1R21EB008154-01A1. We also gratefully acknowledge the support of a Kirck grant from Purdue University.

References

1. X. D. Fan, I. M. White, S. I. Shopoua, H. Y. Zhu, J. D. Suter, and Y. Z. Sun, Anal. Chim. Acta **620**, 8 (2008).
2. D. D. Nolte, Rev. Sci. Instrum. **80**, 101101 (2009).
3. D. D. Nolte, *Optical Interferometry for Biology and Medicine* (Springer, 2011).
4. Y. G. Tsay, C. I. Lin, J. Lee, E. K. Gustafson, R. Appelqvist, P. Magginetti, R. Norton, N. Teng, and D. Charlton, Clin. Chem. **37**, 1502 (1991).
5. J. B. Goh, P. L. Tam, R. W. Loo, and M. C. Goh, Anal. Biochem. **313**, 262 (2003).
6. R. W. Loo, P. L. Tam, J. B. Goh, and M. C. Goh, Anal. Biochem. **337**, 338 (2005).
7. R. M. Ostroff, D. Hopkins, A. B. Haeberli, W. Baouchi, and B. Polisky, Clin. Chem. **45**, 1659 (1999).
8. T. Gao and L. J. Rothberg, Anal. Chem. **79**, 7589 (2007).
9. M. Zhao, X. Wang, and D. D. Nolte, Opt. Express **16**, 7102 (2008).
10. E. Ozkumur, J. W. Needham, D. A. Bergstein, R. Gonzalez, M. Cabodi, J. M. Gershoni, B. B. Goldberg, and M. S. Unlu, Proc. Natl. Acad. Sci. USA **105**, 7988 (2008).
11. X. F. Wang, M. Zhao, and D. D. Nolte, Appl. Opt. **46**, 7836 (2007).
12. X. F. Wang, M. Zhao, and D. D. Nolte, Appl. Phys. Lett. **93**, 223904 (2008).